Appendix

Contents

A.1. Strategy for Anatomical Brain Region Selection in Relevance Bias

Alzheimer's Disease (AD) is a progressive neurological disorder characterized by the deterioration of cognitive functions, particularly memory. A key pathological hallmark of AD is the accumulation of abnormal tau proteins inside neurons, forming structures known as *neurofibrillary tangles*. These tangles disrupt normal neuronal function and lead to cell death. The progression of tau pathology follows a predictable pattern in the brain, described by Braak and Braak staging [9], which correlates with the severity of clinical symptoms.

As tau pathology advances, it causes structural changes in the brain that can be detected by sMRI. These changes, referred to as *sMRI markers*, include the thinning of cortical regions and the shrinkage (atrophy) of specific brain structures due to the loss of neurons and synapses [44]. The microscopic view of the same is elaborated in Figure A6.

Our study selected 50 brain regions (parcels) from the AAL3 atlas and 31 regions (parcels) from the JHU White Matter atlas based on their high relevance to AD. These regions are known to be affected by tau pathology and exhibit measurable changes (albeit few showing minuscule changes) in sMRI scans, making them critical for developing computational models to detect and monitor AD progression. The rest of the brain volume is considered to be low-relevance regions. The details of the regions selected for their relevance to AD are elaborated in Table A3.

All selected high-relevant regions are visualized in Figure A6. The volume ratio between high and low relevance regions varies across stages by downsampling due to max-pooling operations (Section 3.1) to align spatially with the input data at each stage. Relevance regions' volumetric variations across the stages are captured in Figure A7.

A.2. Strategy for Anatomical Brain Region Selection for Generation of Masks

We divided the brain into 10 sub-masks (Mask 1–Mask 10) Table A5 by synthesizing neuropathological staging of Alzheimer's disease (AD) [5, 9], longitudinal biomarker trajectories [7, 32], and structural MRI (sMRI)-visible atrophy patterns [22, 39]. The segregation prioritizes regions vulnerable to tau pathology [16] and amyloid-β deposition [7] while ensuring visibility of degeneration on sMRI for computational modeling [19, 44]. Early-stage masks (Mask 1 – Mask 3) focus on medial temporal and limbic structures, aligning with Braak staging [9] and hippocampal atrophy [41, 42]. Mid-stage masks (Mask 4 – Mask 7) target parietal and frontal association cortices, reflecting default mode network (DMN) disintegration [10, 49] and cortical thinning in angular/supramarginal gyri [4]. Late-stage masks (Mask 8 – Mask 10) include occipital, cerebellar, and sensorimotor regions to capture widespread neurodegeneration [34] and differentiate AD from comorbidities [18].

White matter tracts (e.g., fornix, cingulum) were incorporated based on their disconnection roles in early AD [11, 23], while subcortical nuclei (e.g., caudate, pallidum) were retained for vascular co-pathology analysis [15]. Parcellation leveraged the AAL3 atlas (170 regions [56]) and JHU white matter atlas (48 tracts [6, 40]), ensuring compatibility with clinical diagnostic frameworks [40]. This hierarchical design balances neuropathological specificity [5] with sMRI-driven visibility [22], enabling models to learn atrophy patterns tied to AD progression [32] while accounting for mixed pathologies [16].

A.3. "Reverse" Leave-One-Out: Keeping Only the Masked Region

To complement the Leave-one-out approach discussed in this work, we also inverted the masking procedure—feeding only the sub-masked regions (e.g., Mask 1 alone, Mask 2 alone, etc.) to the Rel-SA model while zeroing out the rest of the brain. Under this setting, one might expect that clinically high-priority regions (like Mask 1) would yield higher performance on their own, showing a smaller drop relative to the baseline model, whereas lower-relevance regions (e.g., Mask 10) would produce larger performance gaps. Indeed, in the attached ROC curve, Mask 1 alone achieves the best AUC among these partial-volume inputs (AUC $\approx$ 0.66), whereas Mask 10 alone drops to around 0.44. Refer to Figure A9 for visualization of attention rollout of the same overlayed on the original MRI input and the masked region input for better interpretation.

This again highlights that, without the targeted attention introduced by Rel-SA, the ViT might be compensating in ways that do not strictly align with clinical expectations.

Table A3. This table depicts regions of High Relevance across the Brain volume in AD pathology from AAL3 and JHU_WM Atlases along with the justification for their selection.

No.	Region and Parcel Numbers	Definition and Justification
1	Hippocampus Left & Right (AAL3: 41, 42)	The hippocampus is essential for forming new memories and spatial orientation. One of the earliest regions affected by tau pathology (Braak stages I-II). Tau accumulation leads to neuronal loss and atrophy, which are visible on sMRI as reduced hippocampal volume. This atrophy correlates with memory deficits, a primary symptom of AD [44].
2	Parahippocampal Gyrus Left & Right (AAL3: 43, 44)	Grey matter cortical region of the brain surrounding the hippocampus; involved in memory encoding and retrieval. Tau pathology begins here during the initial stages of AD (Braak stages I-II). Atrophy disrupts communication with the hippocampus, worsening memory impairments. sMRI shows cortical thinning in early AD [9].
3	Amygdala Left & Right (AAL3: 45, 46)	Processes emotions and emotional memories. Affected in Braak stages III-IV. Tau accumulation contributes to emotional disturbances and neuropsychiatric symptoms. sMRI reveals amygdalar atrophy correlating with symptom severity [44].
4	Fusiform Gyrus Left & Right (AAL3: 59, 60)	Involved in high-level visual processing, such as facial and object recognition. Tau pathology affects this region in Braak stages III-IV. Degeneration in this cortical region leads to difficulties in recognizing faces and objects. sMRI detects cortical thinning in AD patients.
5	Inferior Occipital Gyrus Left & Right (AAL3: 57, 58)	Plays a role in visual perception and processing. In later AD stages (Braak stages V-VI), tau pathology spreads here, causing visual processing deficits. sMRI shows structural changes associated with these deficits.
6	Superior Frontal Gyrus Left & Right (AAL3: 3, 4)	Associated with attention, working memory, and decision-making. Tau pathology reaches the frontal lobes in advanced AD stages (Braak stages V-VI). Atrophy leads to impairments in executive functions, observable in sMRI as cortical thinning [44].
7	Rectus Gyrus Left & Right (AAL3: 23, 24)	Part of the orbitofrontal cortex involved in emotion regulation and social behaviour. Degeneration affects emotional processing and decision-making abilities. sMRI detects atrophy in intermediate to advanced AD stages.
8	Orbitofrontal Cortex Posterior & Lateral Left & Right (AAL3: 29-32)	Involved in reward processing, impulse control, and decision-making. Tau pathology contributes to behavioural changes in AD, such as apathy and disinhibition. sMRI shows volume loss correlating with these symptoms.
9	Middle Cingulate Cortex Left & Right (AAL3: 37, 38)	Involved in cognitive control and pain processing. Early tau pathology (Braak stages III-IV) affects these regions, disrupting cognitive functions. sMRI reveals atrophy correlating with declines in attention and memory.
10	Posterior Cingulate Cortex Left & Right (AAL3: 39, 40)	Involved in memory retrieval; central node in the default mode network. Early involvement leads to disrupted network connectivity and cognitive decline. sMRI shows atrophy correlating to these regions in AD patients.
11	Anterior Cingulate Cortex Subgenual & Prelimbic Left & Right (AAL3: 151-154)	Involved in emotional regulation and cognitive control. Degeneration contributes to deficits in attention and executive function. sMRI shows structural changes in these regions associated with disease progression.
12	Insula Left & Right (AAL3: 33, 34)	Involved in consciousness, emotion, and homeostasis. Early tau pathology leads to deficits in emotional awareness and social cognition. sMRI detects such structural changes.
13	Angular Gyrus Left & Right (AAL3: 69, 70)	Integrates sensory information; important for language and number processing. Affected in Braak stages V-VI. Tau pathology leads to language difficulties and mathematical problems. sMRI detects cortical thinning associated with these impairments.
14	Precuneus Left & Right (AAL3: 71, 72)	Involved in aspects of consciousness and self-reflection. Early involvement by tau pathology leads to deficits in memory and visuospatial skills. sMRI shows atrophy of these regions in AD patients.
15	Caudate Nucleus Left & Right (AAL3: 75, 76)	Plays a role in motor processes and learning. Tau accumulation contributes to motor dysfunctions in AD. sMRI reveals volume reduction correlating with disease severity.
16	Putamen Left & Right (AAL3: 77, 78)	Involved in regulating movements and various types of learning. Degeneration affects motor skills and procedural learning. sMRI indicates atrophy in these regions in advanced AD stages.
17	Pallidum Left & Right (AAL3: 79, 80)	Involved in regulation of voluntary movement. Structural changes contribute to motor symptoms in late-stage AD, detectable via sMRI.
18	Thalamic Nuclei Left & Right (AAL3: 121-132)	Acts as a relay station for sensory and motor signals to the cortex. Tau pathology affects these nuclei in advanced AD, leading to widespread cognitive deficits. sMRI shows thalamic atrophy correlating with disease progression.
19	Nucleus Accumbens Left & Right (AAL3: 157, 158)	Part of the reward circuit; involved in motivation and reinforcement learning. Degeneration contributes to apathy and decreased motivation in AD patients. sMRI shows volume loss associated with these symptoms.
20	Genu of Corpus Callosum (JHU WM: 4)	Connects the frontal lobes of the two hemispheres. Degeneration leads to disrupted interhemispheric communication, affecting cognitive functions. sMRI and DTI detect changes in fiber integrity in AD.
21	Body of Corpus Callosum (JHU WM: 5)	Connects the motor, sensory, and parietal cortex between hemispheres. Degeneration leads to motor and sensory deficits due to disrupted communication. Detectable via sMRI and DTI.
22	Splenium of Corpus Callosum (JHU WM: 6)	Connects the occipital lobes, facilitating visual information exchange. Degeneration leads to visual processing deficits. sMRI and DTI show decreased integrity in AD patients.
23	Fornix (Cres) (JHU WM: 7), Fornix (Body) (JHU WM: 40), Fornix (Cres) (JHU WM: 41)	Connects the hippocampus to other parts of the limbic system. Early degeneration correlates with memory loss in AD. DTI shows reduced integrity of fornix fibers.
24	Medial Lemniscus Left & Right (JHU WM: 10, 11)	Carries sensory information from the spinal cord to the brain. Although not traditionally emphasized in AD, degeneration may contribute to sensory deficits. Detectable via sMRI.
25	Anterior Limb of Internal Capsule Left & Right (JHU WM: 18, 19)	Connects frontal cortex with subcortical structures. Degeneration affects cognitive functions like decision-making and executive function. DTI detects changes in these regions in AD.
26	Posterior Limb of Internal Capsule Left & Right (JHU WM: 20, 21)	Connects motor cortex with spinal cord and subcortical structures. Degeneration leads to motor deficits. Detectable via sMRI and DTI.
27	Retrolenticular Part of Internal Capsule Left & Right (JHU WM: 22, 23)	Contains optic radiation fibers connecting thalamus to the visual cortex. Degeneration leads to visual processing deficits. DTI shows changes in fiber integrity.
28	Anterior Corona Radiata Left & Right (JHU WM: 24, 25)	Connects frontal cortex to the brainstem. Structural changes contribute to cognitive deficits. sMRI and DTI detect decreased white matter integrity.
29	Posterior Corona Radiata Left & Right (JHU WM: 28, 29)	Connects parietal and occipital lobes to the brainstem. Degeneration leads to sensory and visual processing deficits. Detectable via sMRI and DTI.
30	Posterior Thalamic Radiation Left & Right (JHU WM: 30, 31)	Connects thalamus with occipital cortex; includes optic radiations. Degeneration leads to visual deficits. DTI shows white matter changes in AD.
31	External Capsule Left & Right (JHU WM: 34, 35)	Connects cerebral cortex with basal ganglia. Degeneration may disrupt cortical-subcortical communication. sMRI reveals structural changes.
32	Cingulum Left & Right (JHU WM: 36, 37)	Connects cingulate gyrus with hippocampus and other regions. It is affected in early AD stages, leading to cognitive impairments. sMRI and DTI reveal structural changes.
33	Cingulum (Hippocampus) Left & Right (JHU WM: 38, 39)	Specific part of cingulum connecting to the hippocampus. Degeneration impacts memory and spatial navigation. Detectable via sMRI and DTI.
34	Superior Longitudinal Fasciculus Left & Right (JHU WM: 42, 43)	Connects frontal lobe with parietal, occipital, and temporal lobes. They are affected by AD, leading to deficits in language and attention. DTI shows reduced integrity.
35	Superior Fronto-Occipital Fasciculus (JHU WM: 44)	Connects frontal lobe with occipital lobe. Degeneration affects executive functions and visuospatial processing. Structural changes are detectable via DTI.
36	Uncinate Fasciculus Left & Right (JHU WM: 45, 46)	Connects anterior temporal lobe with orbitofrontal cortex. Early involvement leads to impairments in memory and social cognition. DTI reveals decreased fiber integrity.

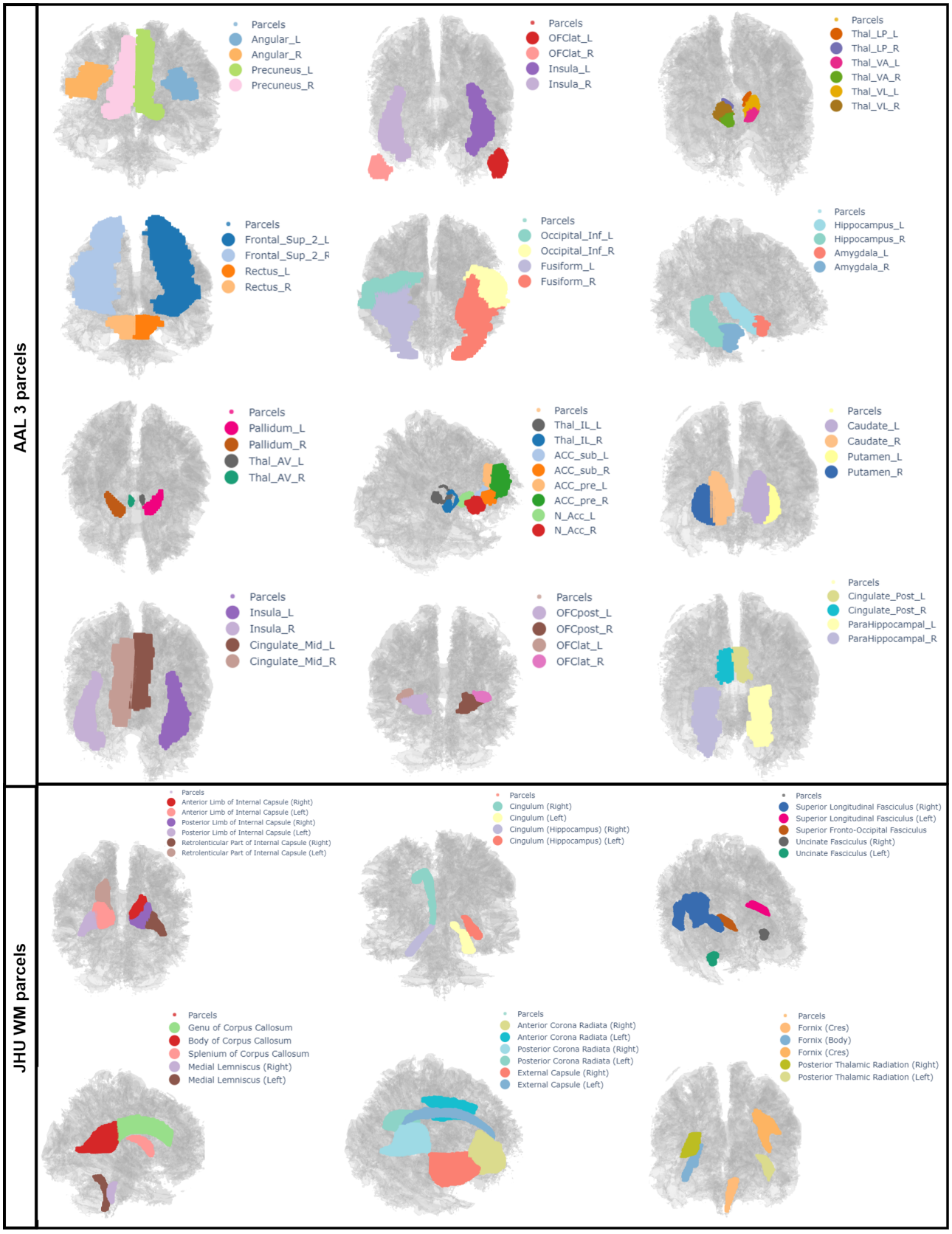

Figure A6. Regions affected in AD pathology are identified as Parcels of High Relevance from AAL3 and JHU-WM Atlases; Parcels are visualized as segregated Groups to avoid cluttering and overlapping of regions.

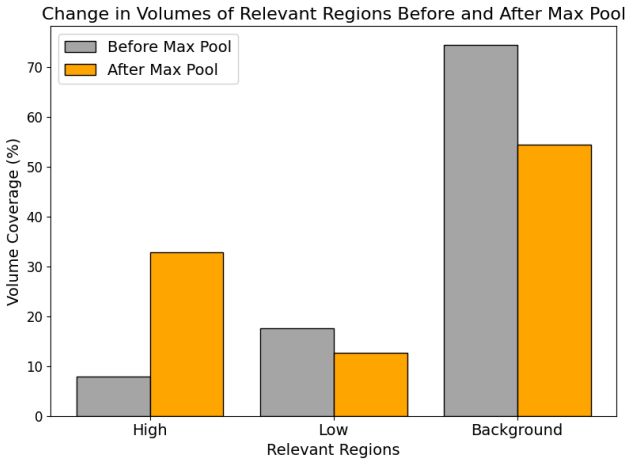

Figure A7. Volumetric Coverage of Background, High and Low Relevant Regions before and after max-pooling of a single subject's sMRI scan for generation of masks for Rel-SA module.

Table A4. Model training Configuration and Hyperparameters for training 2-class classification on ADNI/AIBL dataset.

Hyperparameter	**Value**
# Parameters	95,867,546
Device	CUDA
Batch Size	16
Patch Size (p_D, p_W, p_H)	(16,16,16)
# Epochs	30
# Transformer blocks	12
# Heads	12
Loss Function	Cross Entropy Loss
Optimizer	AdamW
Learning Rate	1e-4
Weight Decay	1e-4
Scheduler	Warmup+CosineAnnealingLR
Minimum Learning Rate	1e-6
T_max	35

Table A5. Overview of the 10-Mask Configuration for Leave-One-Out analysis. Each mask groups brain parcels based on anatomical relevance to Alzheimer's Disease (AD). The table summarizes: relevance to AD, visibility in sMRI scans, AAL3v1 parcel IDs, and associated brain regions.

Mask	**AD Relevance**	**sMRI Visibility**	**AAL3 Parcel IDs**	**JHU Parcel IDs**	**Brain Regions Included**
Mask1	Very High	High	41, 42, 43, 44, 45, 46, 21, 22, 59, 60, 67, 68, 83, 84, 85, 86, 81, 82, 23, 24, 151, 152	45, 46, 40, 7, 41, 38, 39	Hippocampus, parahippocampal gyrus, amygdala, olfactory cortex, fusiform gyrus, temporal poles, rectus gyrus, subgenual ACC, uncinate fasciculus, fornix, cingulum (hippocampus)
Mask2	High	Moderate-High	39, 40, 71, 72	36, 37	Posterior cingulate, precuneus, cingulum (cingulate gyrus)
Mask3	Moderate	Moderate	35, 36, 89, 90	None	Pregenual ACC, medial frontal cortex
Mask4	Moderate	Moderate	69, 70, 63, 64	None	Angular gyrus, supramarginal gyrus
Mask5	Moderate	Moderate	105, 106, 153, 154	None	Superior parietal lobule, supracallosal ACC
Mask6	Low	High	53, 54, 55, 56, 57, 58, 51, 52	30, 31, 32, 33, 47, 48	Occipital cortex (superior, middle, inferior), lingual gyrus, posterior thalamic radiation, sagittal stratum, tapetum
Mask7	Low-Moderate	Moderate-High	7, 8, 17, 18, 25, 26, 33, 34	18, 19, 24, 25, 4	Superior/middle frontal cortex, supplementary motor area, insula, anterior limb of internal capsule, anterior corona radiata, genu of corpus callosum
Mask8	Low	Low	93, 94, 95, 96, 15, 16, 13, 14, 11, 12, 65, 66, 75, 76, 77, 78, 79, 80	None	Inferior frontal cortex (orbital, opercular, triangular), superior temporal gyrus, caudate, putamen, pallidum
Mask9	Low	High	47, 48, 49, 50, 121, 122	6	Calcarine cortex, cuneus, thalamus, splenium of corpus callosum
Mask10	Low	High	1, 2, 5, 6, 73, 74, 61, 62, 167, 168, 169, 170, 97–166 (cerebellar regions)	5, 8, 9, 26, 27, 20, 21, 10, 11, 16, 17, 2, 3	Precentral/postcentral gyri, paracentral lobule, Heschl's gyrus, midbrain, pons, medulla, cerebellum (all regions), corticospinal tract, superior corona radiata, posterior limb of internal capsule, medial lemniscus, cerebral peduncle, middle cerebellar peduncle, pontine crossing tract

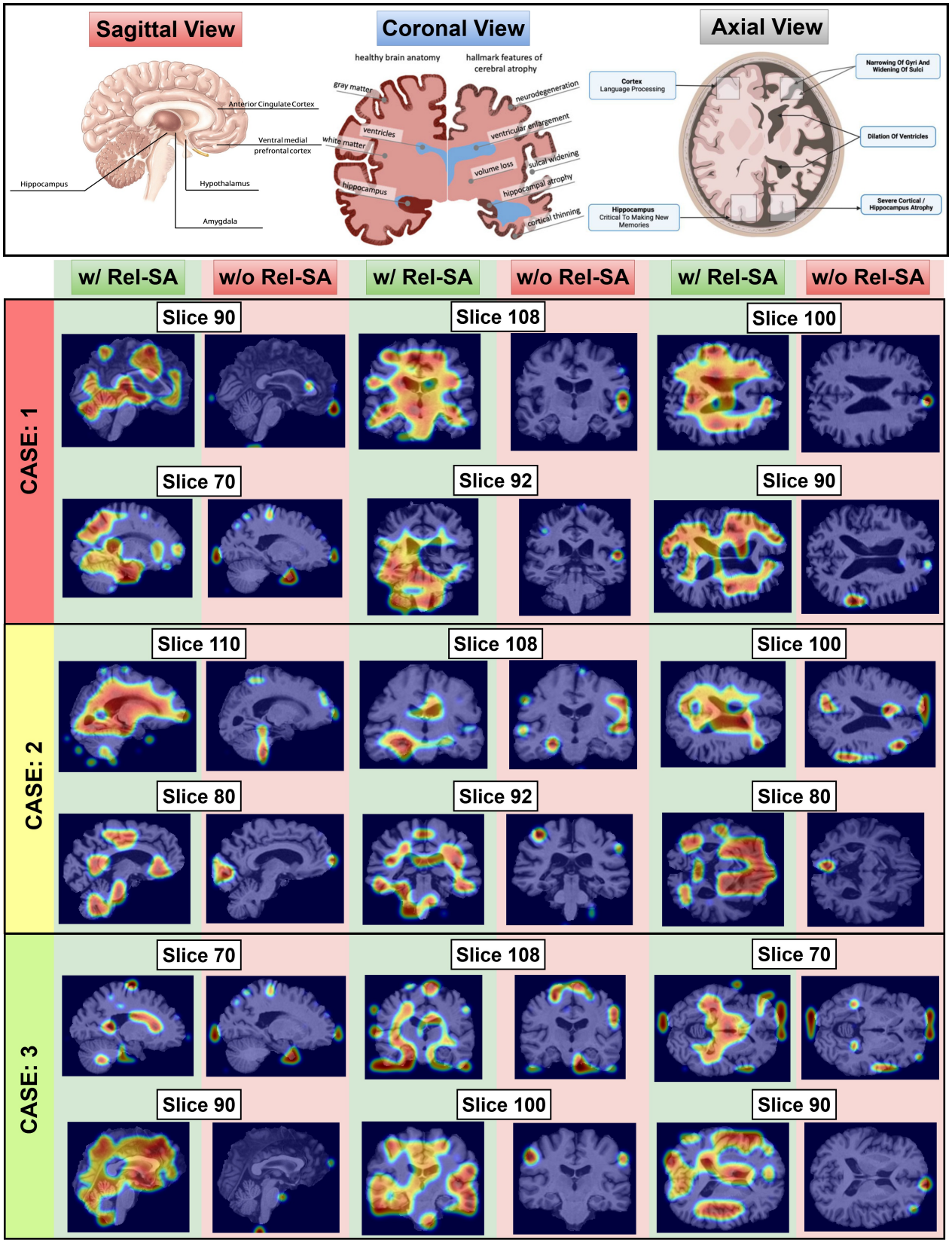

Figure A8. 2D slice-wise attention rollout visualization across three representative cases. Case 1: Ground truth AD, predicted as AD by both models. Case 2: Ground truth AD, predicted as CN by vanilla ViT but predicted AD (correct) by ViT with Rel-SA. Case 3: Ground truth CN, predicted as CN by both models. Top-labeled slices across sagittal, coronal, and axial views indicate regions typically affected by AD for anatomical reference. The representative slices are sourced from [8, 50] and https://o.quizlet.com/41IohmVEJxrSq67GZd8H8w_b.png

.

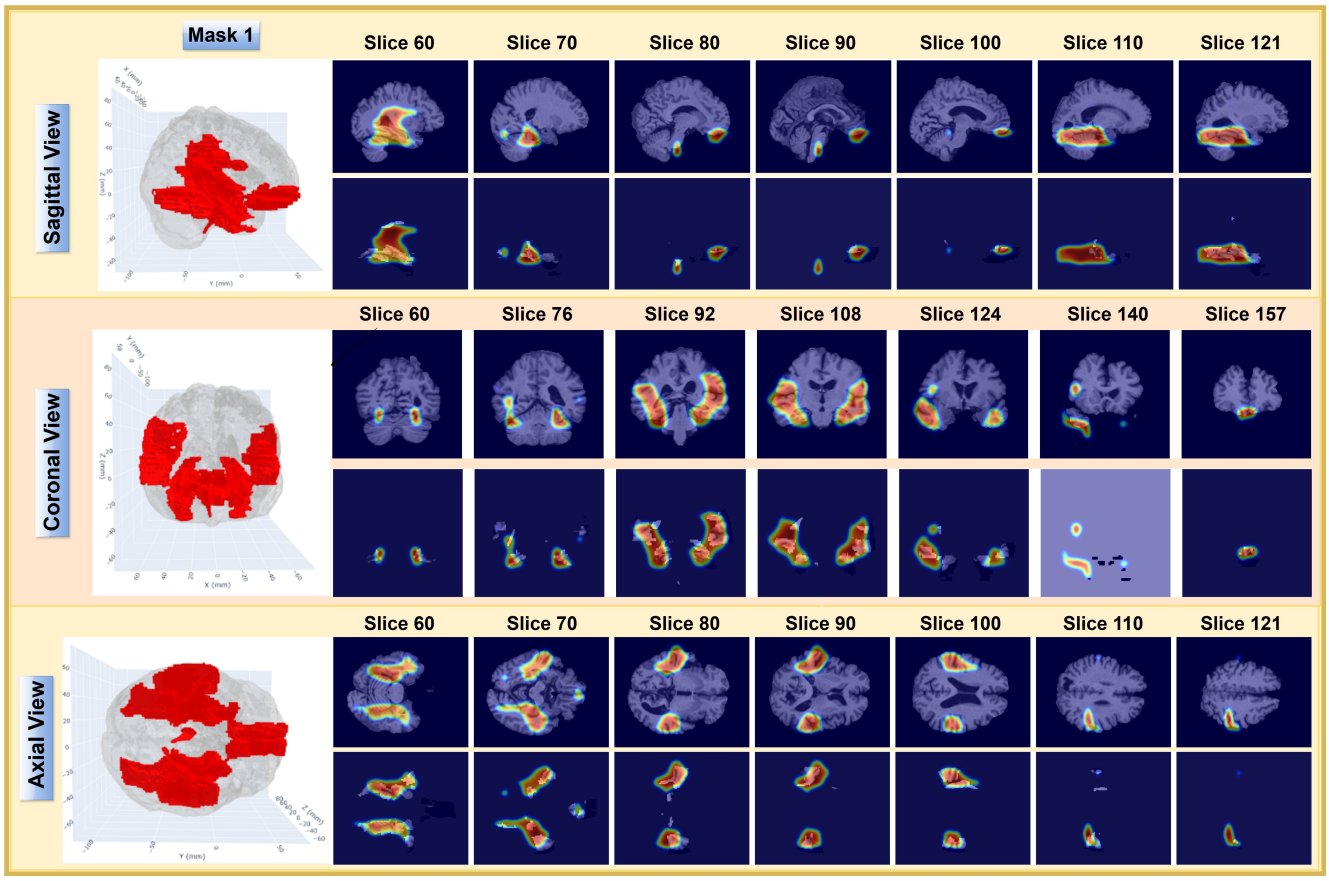

Figure A9. Attention rollout visualization for a correctly predicted Alzheimer's Disease (AD) sample using the proposed Rel-SA module during Reverse Leave-One-Out analysis with only Mask 1 region as input. The top row in each view shows the attention rollout overlaid on the original brain image, helping readers visually localize the focused regions in anatomical context. As expected, the attention is predominantly concentrated within the Mask 1 region. The bottom row displays only the Mask 1 region across the slices, highlighting the exact input provided to the model.